Available online at www.sciencedirect.com
SCIENCE DIRECT
Journal of the European Ceramic Society 26 (2006) 1663–1671
www.elsevier.com/locate/jeurceramsoc

Porous ceramic supports for membranes prepared from kaolin and doloma mixtures

F. Bouzerara [a], A. Harabi [a,*], S. Achour [a], A. Larbot [b]

[a] *Constantine Ceramics Laboratory, Mentouri University, Constantine 25000, Algeria*
[b] *Institut Européen des Membranes, UMR 5635 CNRS ENSCM UMII, 1919 Route de Mende, 34293 Montpellier Cedex 5, France*

Received 5 August 2004; received in revised form 27 February 2005; accepted 12 March 2005
Available online 10 May 2005

Abstract

The present paper reports the in situ synthesis of porous ceramic supports from local kaolin and kaolin–doloma mixtures. These raw materials have been dictated by their natural abundance (low price) and their beneficial properties. In this work, four different processing routes have been presented. In addition, two support shapes are of particular interest: tubular and flat configurations, which are currently the most used supports in membrane research. Tubular configurations have been produced by extrusion method whereas flat configurations have been produced by both dry-pressing and roll pressing. The doloma addition to kaolin has a positive effect on the porosity ratio of supports compared to those prepared from kaolin alone. Moreover, the influence of the sintering temperature on the total porosity, average pore size, pore size distribution and strength of supports has been investigated. It has been found that higher sintering temperatures (1250 °C) were needed to obtain a uniform pore size distribution within total porosity ratios of 43 and, 51% when processes 3 and 2 were applied, respectively.

Keywords: Kaolin; Membranes; Strength; Porosity; Extrusion

1. Introduction

Due to their potential application in a wide range of industrial processes, membrane technologies have received an increasing interest. Ultrafiltration and microfiltration are often used to remove particles, microorganism, and colloidal materials from suspensions.[1,2] The use of ceramic membranes has many advantages such as high thermal and chemical stability,[3–5] pressure resistance, long lifetime, and catalytic properties from their intrinsic nature.[1] A membrane support provides mechanical strength to a membrane top-layer to withstand the stress induced by the pressure difference applied over the entire membrane and must simultaneously have a low resistance to the filtrate flow.

The marketed supports are generally manufactured from compounds such as alumina (Al_2O_3), cordierite ($2MgO{\cdot}2Al_2O_3{\cdot}5SiO_2$) and mullite ($3Al_2O_3{\cdot}2SiO_2$),[3,5–8] which have a relatively elevated cost. In order to decrease this cost and to evaluate our natural resources,[9,10] the supports have been manufactured, in this work, from kaolin ($Al_2O_3{\cdot}2SiO_2{\cdot}2H_2O$) and the mineral dolomite ($CaMg(CO_3)_2$) local raw materials. The doloma powder (phase mixture of MgO and CaO) was obtained from dolomite by calcination at 900 °C.

Generally, membrane supports should have a total porosity ratio of about 45%. A preliminary work carried out on the sintering of kaolin[11] (process 1, in this study) showed that it was difficult to reach the required porosity ratio. Therefore, the doloma was added into kaolin (processes 2, 3 and 4, in the present study) to slow down its sinterability. Previous studies on doloma-based ceramics showed that their sintering was very difficult, unless the doloma powder was activated by a proposed process, described in Ref. [12]. For example, it was found that the density of doloma samples sintered at 1200 °C for 2 h was about 43% of the theoretical, using the non-treated doloma. In contrast to this, when the doloma activated fine powder was used, a 90% of the theoretical density

* Corresponding author. Tel.: +213 31 614785; fax: +213 31 614785.
E-mail address: harabi52@hotmail.com (A. Harabi).

0955-2219/$ – see front matter © 2005 Elsevier Ltd. All rights reserved.
doi:10.1016/j.jeurceramsoc.2005.03.244

was achieved under the same conditions of sintering. Consequently, 15.0 wt% of doloma has been added into kaolin to obtain porous ceramic supports for membranes, in this work.

2. Experimental procedures

2.1. Analysis of the raw materials

The starting raw materials were domestic kaolin and dolomite derived from Guelma and Batna regions (Algeria), respectively.

The chemical composition of kaolin given in weight percentages of oxides is given in Table 1, where the main impurities are CaO, MnO and Fe_2O_3. The particle size distribution of this material was determined by the Dynamic Laser Beam Scattering (DLBS) technique (Fig. 1). This method gave an average particle size in the order of 9.6 μm.

The doloma (CaO·MgO) has been obtained from dolomite after calcination at 950 °C for 4 h.

The purity of the added doloma is about 99.6 wt%. It contains, mainly, 0.27 wt% Fe_2O_3, 0.07 wt% Al_2O_3 and 0.02 wt% Na_2O as purities.

Fig. 2 shows XRD spectrum of doloma powder, where only CaO and MgO are present. This spectrum shows also that the doloma powder is well crystallized. The average particle size of this powder has been estimated from XRD spectra,

Table 1
Chemical composition of kaolin (wt%), using fluorescence XRD analysis

Oxides	wt%
Al_2O_3	37.27
SiO_2	43.69
CaO	00.38
MgO	00.06
MnO	00.41
Fe_2O_3	00.64
TiO_2	00.09
I.L.	17.46

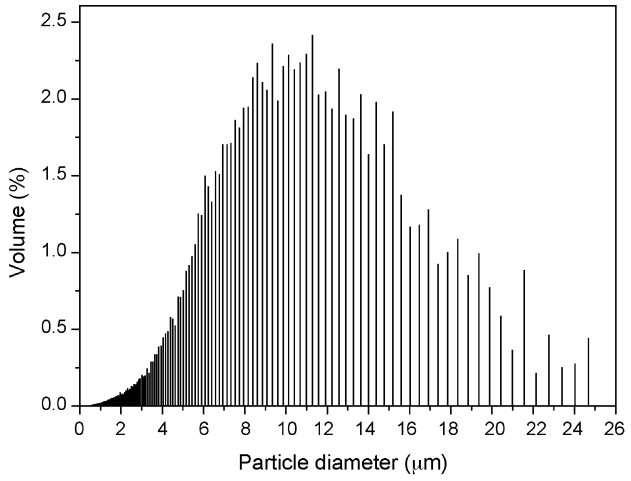

Fig. 1. Particle size distribution of kaolin powder, used in this work.

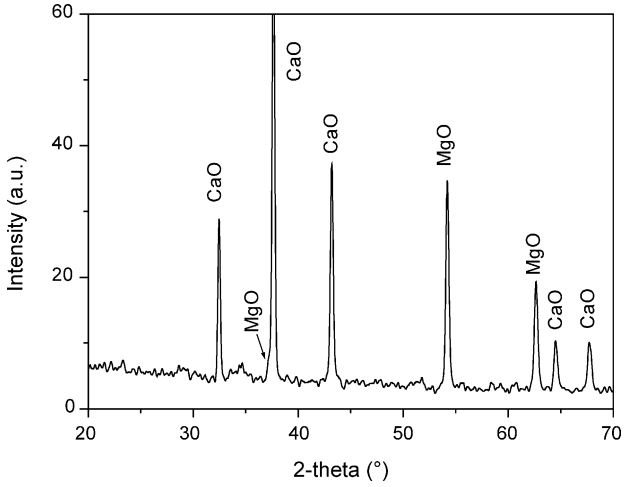

Fig. 2. XRD spectrum of doloma powder, obtained from dolomite after calcination at 950 °C for 4 h.

using Scherrer formula. The calculated values are 5.3 and 5.5 μm, for CaO and MgO, respectively. It should be noticed that the average particle size determined by DLBS technique has not been utilized because of CaO hydration.

2.2. Supports elaboration

The main steps of the four processing routes (noted 1, 2, 3 and 4) for samples preparation, used in this work, are described in Fig. 3. One of the main differences between these processes is the shape of the product. The flat configuration is obtained when processes 1, 2 and 4 were applied while

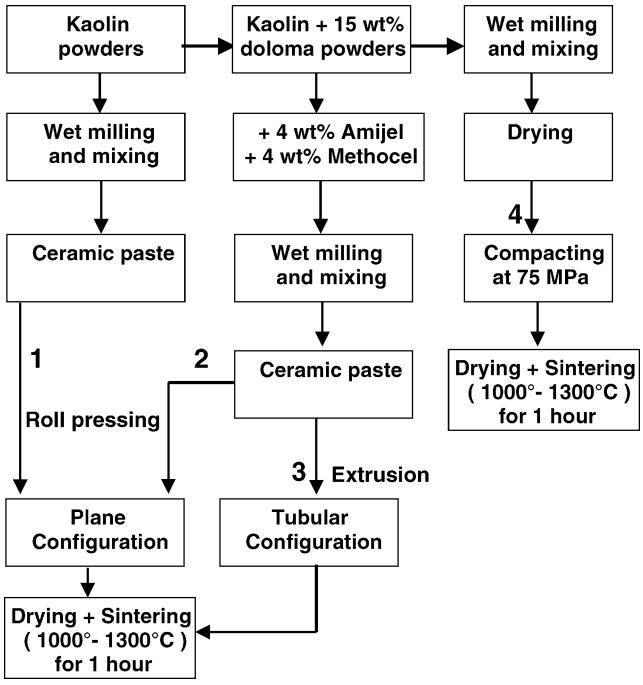

Fig. 3. A schematic diagram showing the main processes (1, 2, 3 and 4), used for membrane supports preparation, in this work.

a tubular one was achieved when process 3 was used. Another important difference is the doloma addition (process 4) and doloma coupled with methocel and amijel additions (processes 2 and 3).

After doloma addition to kaolin, the mixture loses its plastic properties. To improve these properties and facilitate the shaping of products, organic materials have been added (processes 2 and 3). The organic additions used are: 4 wt% of methocel, derived from methylcellulose (The Dow Chemical Company) as a plasticizer and 4 wt% of amijel, derived from starch (Cplus 12072, Cerestar), as a binder.

2.3. Characterization techniques

The structure was analyzed by X-ray diffraction (XRD) and Hg-porosimetry techniques. The presence of possible defects in the prepared supports was checked by using scanning electron microscopy (SEM). The tensile strength testing of sintered samples at room temperature was carried out using the diametral compression test, at a constant displacement rate of 0.2 mm min−1, using hard metal plattens. Generally, three samples of each composition sintered under the same conditions were tested and an average value was taken. Following previous strength testing procedures, packing strips (Manilla office file) of 0.30 mm thickness were used.[13]

3. Results and discussion

3.1. Thermal analysis

Structural evolution of the powder evaluated by thermo gravimetric analysis (TGA) and differential scanning calorimetry (DSC) analysis shows the weight loss of kaolin (K) and kaolin + 15 wt% doloma (KD) mixtures. These two analyses have been carried out under air. The heating rate of the compacts from room temperature to 1200 °C was 10 °C/min, while the cooling of compacts was carried out in the furnace.

TGA curves recorded during compacts heating (Figs. 4 and 5) permit the following remarks. A total weight loss of about 21% of kaolin compacts is measured. In fact, this weight loss consists of two distinct stages. The first one is attributed to the humidity (water added into the starting mixtures) whereas the second stage is related to the departure of water (by vaporization) existing in the kaolin chemical composition itself. The weight loss ratio of the last stage is more pronounced (Fig. 4).

A further weight loss is observed during KD compacts heating. This weight loss is mainly due to doloma rehydration from (Ca, Mg)$(OH)_2$ to MgO and CaO. This rehydration is characterised by two additional peaks (DSC curve, Fig. 5) appearing at about 440 and 645 °C for MgO and CaO, respectively. It should be mentioned that the total weight loss ratio, for this mixture is much higher than that of K compacts alone (about 30%). These observations are also confirmed by

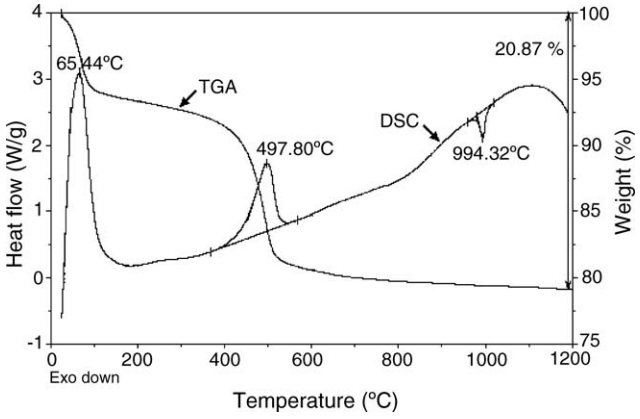

Fig. 4. DSC and TGA curves of kaolin samples.

DSC analysis (Figs. 4 and 5). The two endothermic phenomena, appearing at 65 and 497 °C, correspond to the first and the second stages of weight loss, respectively. A third stage, which is characterized by an exothermic reaction appeared at about 981 °C in both Figs. 4 and 5. It is more remarkable in Fig. 4. The origin of this reaction is not understood yet. Some workers attribute this reaction to spinel formation while others attribute it to mullite nucleation.[13] More possibly, this reaction may be attributed to mullite nucleation, since XRD shows that mullite nucleates first at a relatively lower temperature, before spinel nucleation.

3.2. Phase identification

X-ray diffraction was used to identify the formed phases. In kaolin + doloma materials, heated at 1200 °C, the main observed phases are: mullite ($3Al_2O_3{\cdot}2SiO_2$), cordierite ($2MgO{\cdot}2Al_2O_3{\cdot}5SiO_2$), anorthite ($CaO{\cdot}Al_2O_3{\cdot}2SiO_2$) and spinel ($MgO{\cdot}Al_2O_3$) as shown in Fig. 6. However, for samples sintered at 1300 °C, the mullite phase disappeared. It is worth noting that the total porosity did not change very much with sintering temperatures for a given processing route, apart from the lower sintering temperature (1000 °C). Moreover,

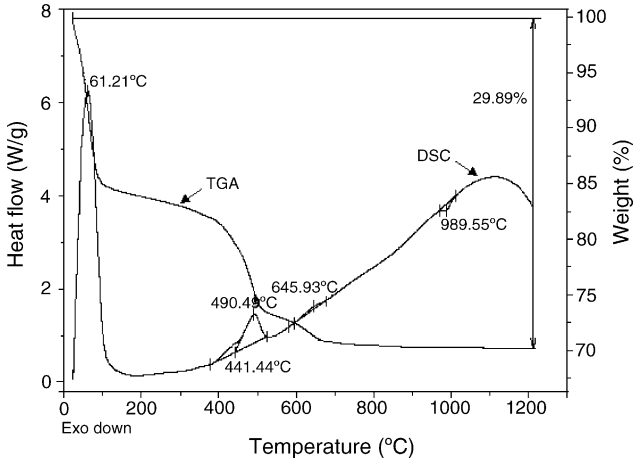

Fig. 5. DSC and TGA curves of kaolin + 15 wt% doloma mixtures.

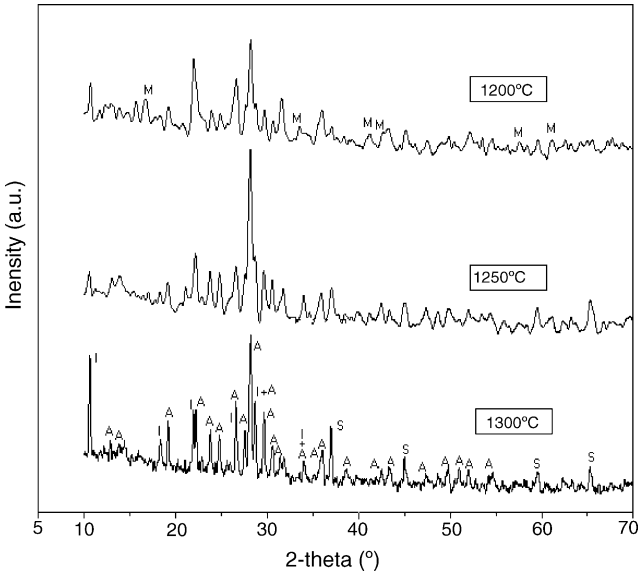

Fig. 6. XRD spectra of kaolin + 15 wt% doloma samples sintered at different temperatures for 1 h. M, Mullite; A, Anorthite; S, Spinel; I, Indialite (α-cordierit).

this means that the porosity is independent of the formed phases. These identified phases are of great importance because of their promising physical and mechanical properties.

3.3. Pore characterization

For the development of high-quality supports, the following properties are of major importance: pore size distribution, total porosity ratio, surface quality with the absence of large defects or large pores, mechanical properties and chemical stability.[3]

Structural characteristics of the final membrane supports, prepared from kaolin and kaolin + doloma, according to the four different processing routes are summarized in Table 2. The total porosity, average pore size and pore size distribution have been determined by mercury intrusion porosimetry for supports sintered at different temperatures for 60 min. The obtained results are illustrated in Figs. 7–10. As would be expected, these figures show, generally that there is an increase in average pore size and a decrease in total porosity in samples, when the sintering temperature is increased. The increase in average pore size is also confirmed by typical micrographs illustrated in Fig. 11.

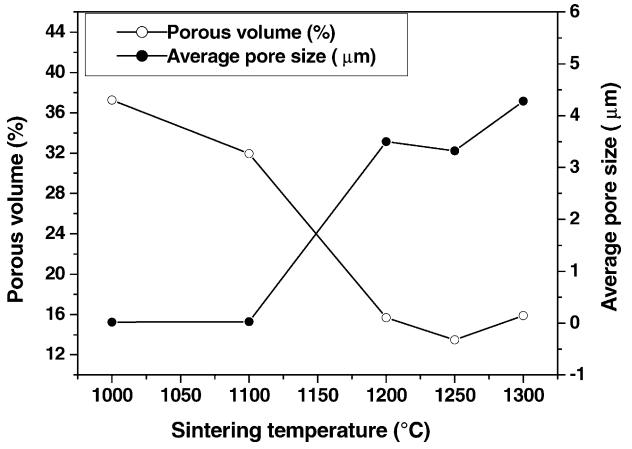

Fig. 7. Porous volume (%) and average pore size vs. sintering temperature for kaolin samples, using process 1.

Moreover, it can be said that both the average pore size and porous volume are closely related to the preparation method. The obtained results (Table 2 and Figs. 7–10) show that the doloma addition to kaolin has a positive effect on the porosity ratio of supports compared to those prepared from kaolin alone. For example, the kaolin support (process 1) had a porosity ratio of ≈13% and an average pore size around 3 μm, whereas the kaolin–doloma supports (process 2) had

Table 2
Some properties of samples prepared from kaolin and kaolin + doloma according to the four different processes

Used processes	Sintering temperature (°C)	Total porosity (%)	A.P.S. (μm)	PSD modal	Tensile strength (MPa)
Process 1	1000	37.26	0.02	BMPSD	
	1200	15.68	3.49	MMPSD	
	1250	13.50	3.32	SMPSD	
	1300	15.94	4.28	SMPSD	
Process 2	1000	56	7.68	MMPSD	
	1200	53.31	12.72	MMPSD	
	1250	51.23	22.31	SMPSD	
	1300	51.9	39.40	SMPSD	
Process 3	1150	39.89	1.65	MMPSD	
	1200	38.29	2.89	BMPSD	
	1250	43.18	27.72	SMPSD	
	1300	40.53	48.93	SMPSD	
Process 4	1000	41.94	0.69	MMPSD	6
	1100	–	–	–	9
	1200	40.99	3.77	SMPSD	15
	1250	40.81	11.09	BMPSD	15
	1300	37.63	23.48	SMPSD	9

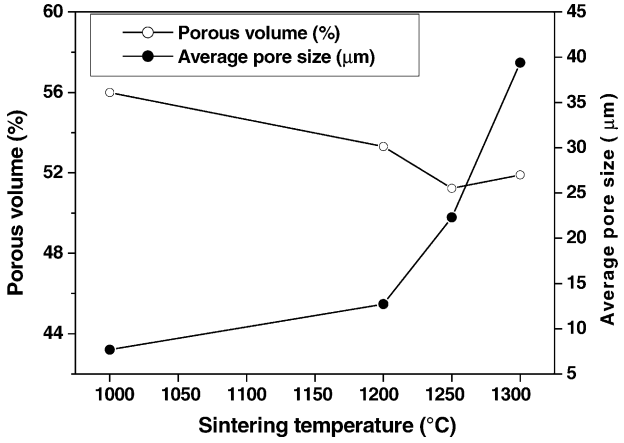

Fig. 8. Porous volume (%) and average pore size vs. sintering temperature for kaolin + 15 wt% doloma samples, using process 2.

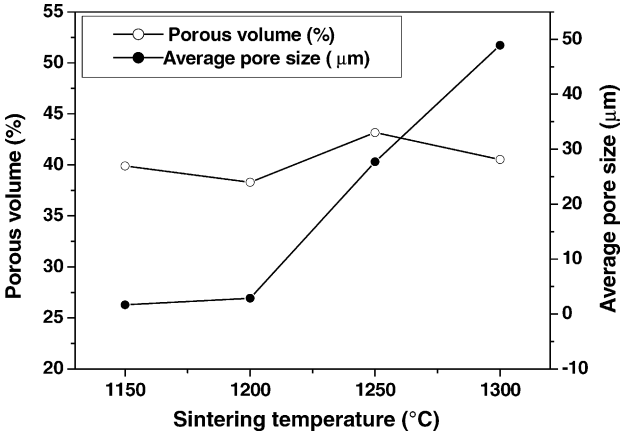

Fig. 9. Porous volume (%) and average pore size vs. sintering temperature for kaolin + 15 wt% doloma samples, using process 3.

a porosity ratio of ≈51% and an average pore size around 22 μm, sintered under the same conditions (1250 °C for 1 h).

As far as preparation processes are concerned, it can be said that doloma addition (processes 2–4) inhibits the sintering of the samples even though at a relatively higher sintering temperature (1300 °C); the total porosity values were between 37 and 56%. On the other hand, the total porosity of samples prepared according to process 1 and sintered at 1200, 1250 and 1300 °C was less than 16%. These results are in good agreement with our results reported elsewhere.[11]

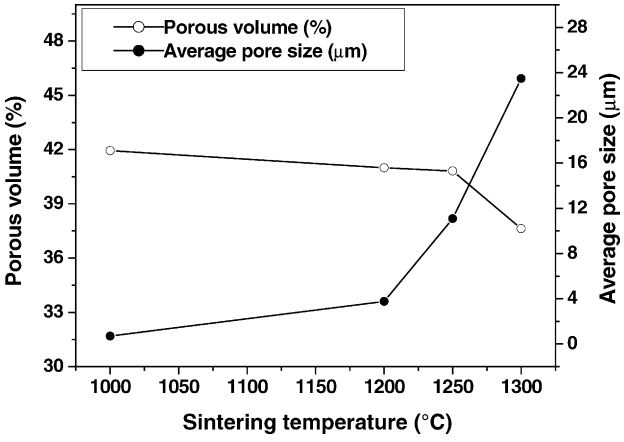

Fig. 10. Porous volume (%) and average pore size vs. sintering temperature for kaolin + 15 wt% doloma samples, using process 4.

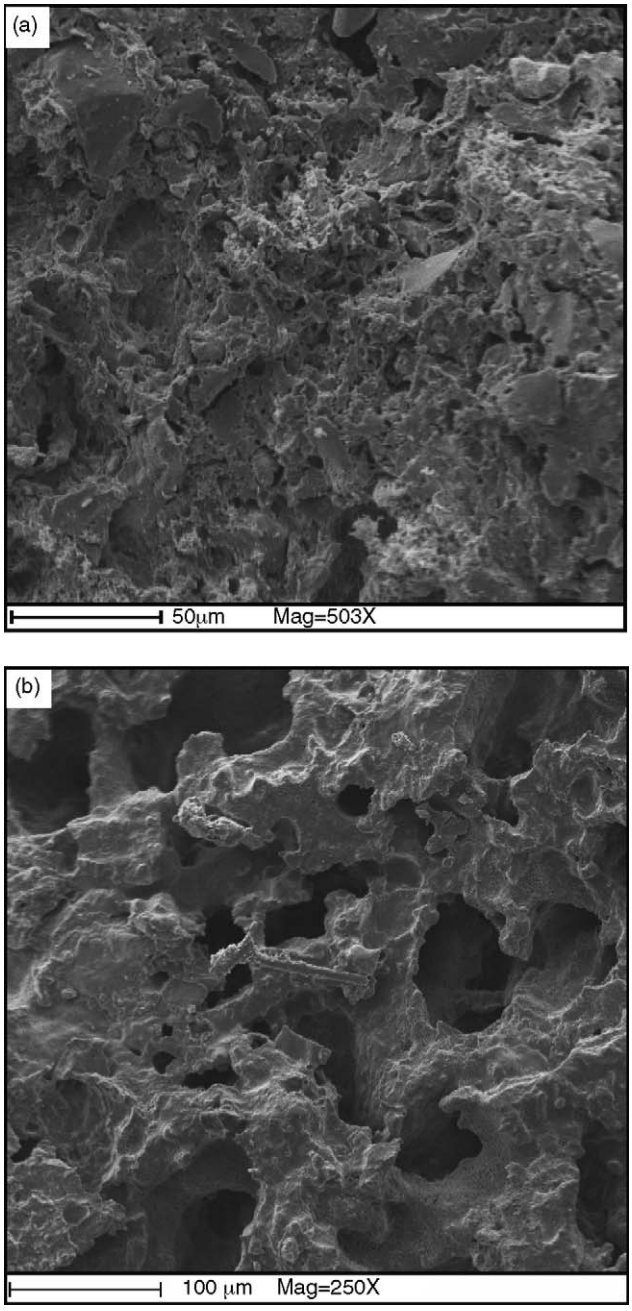

Fig. 11. SEM micrographs of kaolin + 15 wt% doloma samples, using process 3, sintered at 1150 °C (a) and 1250 °C (b).

It has been found that lower doloma additions promote densification while higher doloma additions (10.0 wt%) inhibit the sintering of samples. Thus, the sintering of 100 wt% non-activated doloma powders becomes more difficult. The

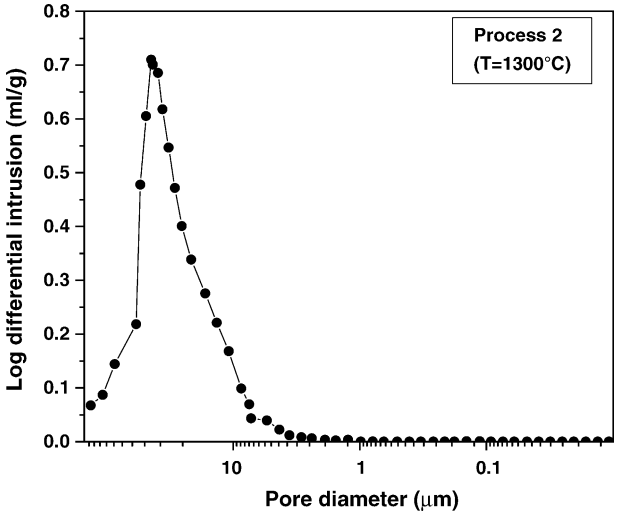

Fig. 12. Pore size distribution in kaolin + 15 wt% doloma samples, using process 2.

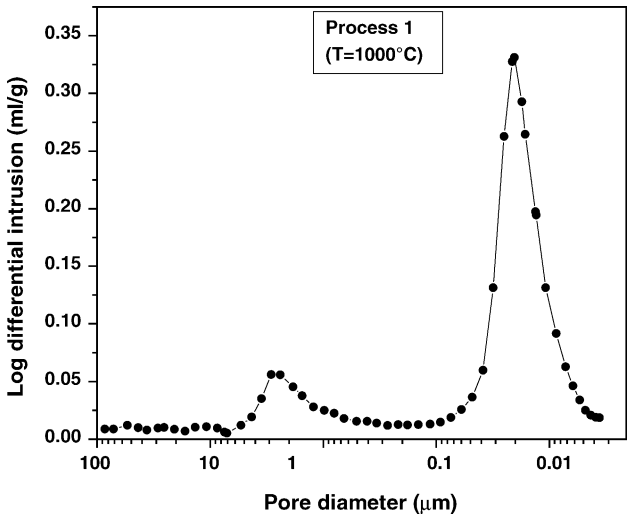

Fig. 13. Pore size distribution in kaolin samples, using process 1.

total porosity ratios for samples prepared according to process 2 are significantly higher than those measured for samples prepared according to processes 3 and 4, under the same sintering conditions. This difference may mainly be due to the weak applied pressure in process 2 (roll pressing), when compared with the values applied for processes 3 and 4 were 10 and 75 MPa, respectively.

The pores characterisation may be divided into three main features (categories). These consist of total porosity, average pore size and the modal distribution of pore size. The pore size distribution modal may also be classified into three distinct modals; single or Gaussian distribution, bi-modal and multi-modal pore size distributions. The single (mono) modal of pore size distribution (SMPSD) is generally obtained for samples having a uniform pore size distribution. When pore volume (%) is plotted against pore size, the curve is characterised by a single peak (Fig. 12). However, the bi-modal of pore size distribution (BMPSD) is characterised by two different or overlapping peaks. This means that there is two classes of pore size distribution (Fig. 13). Finally, the multimodal of pore size distribution (MMPSD) is characterized by the presence of more than two distinct (Fig. 14) or overlapping peaks (Fig. 15).

The BMPSD observed in Fig. 13, using process 1, consists of two different pore origins, existing at this lower sintering temperature (1000 °C). The origin of finer pore sizes may be attributed to the H_2O escaping, while the coarser ones are due to the voids existing between kaolin starting particles. When the sintering temperature is increased (1300 °C), the coalescence of finer pores leads to the disappearance of the second peak (Table 2) and a SMPSD is obtained, within an average pore size of about 4 μm. The BMPSD (mentioned above) becomes MMPSD (Figs. 14 and 16a) when further starting materials have been added such as $Mg(OH)_2$, $Ca(OH)_2$, amijel and methocel, for samples sintered at a lower temperature (1000 °C).

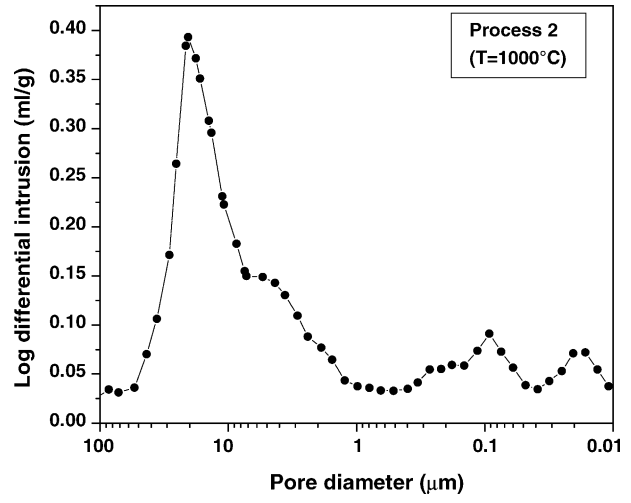

Fig. 14. Pore size distribution in kaolin + 15 wt% doloma samples, using process 2.

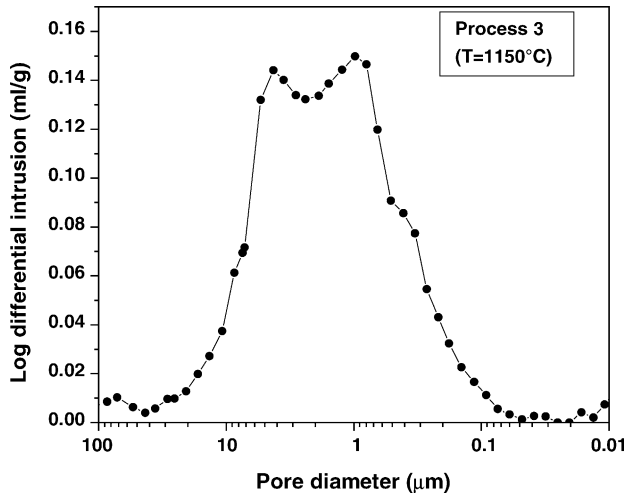

Fig. 15. Pore size distribution in kaolin + 15 wt% doloma samples, using process 3.

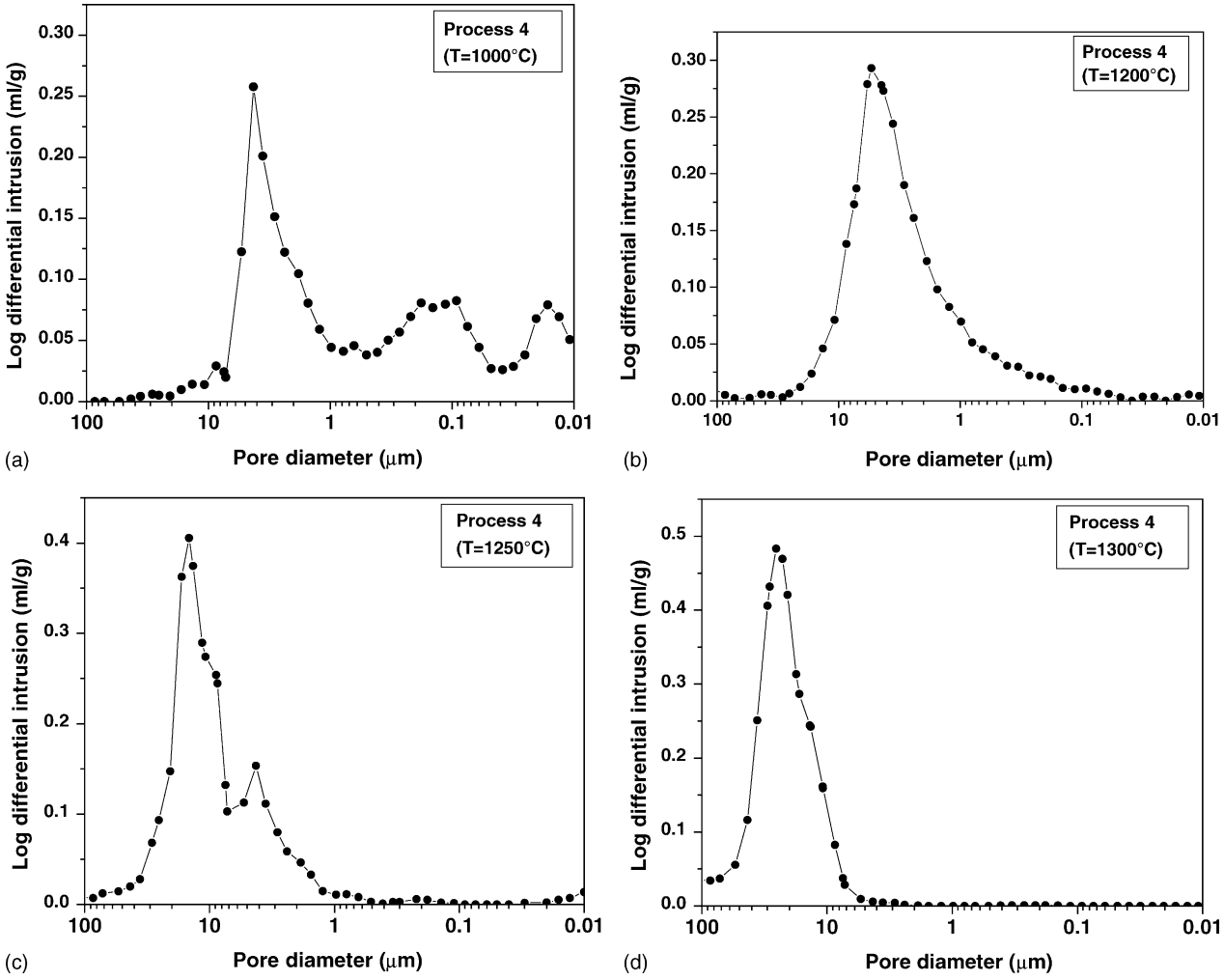

Fig. 16. Pore size distribution in kaolin + 15 wt% doloma samples, using process 4 sintered at different temperatures for 1 h.

Fig. 14 is a good example for that it illustrates well that the number of peaks is about five which corresponds to the number of starting materials (kaolin, $Mg(OH)_2$, $Ca(OH)_2$, amijel and methocel). A uniform pore size distribution (SMPSD) is also obtained when samples were sintered at higher temperature (1300 °C), as shown in Figs. 12 and 16d. Therefore it can be said that these modal distributions are closely related to the processing routes used in this work.

Moreover, the compacting pressure is a major factor controlling the modal distribution of pore size. For example, a uniform pore size distribution is already obtained for samples sintered at 1200 °C (Fig. 16b), using process 4 (75 MPa), while the appearance of this modal is delayed to 1300 °C, using process 2 (hand roll pressing). It should be mentioned that the pore size distribution is almost uniform for samples sintered at 1250 °C for 1 h, using process 4 (Fig. 16c).

Fig. 16 displays the modal distributions of pore size, for samples sintered at different temperatures for 1 h, using process 4. It is clear that the pore size distribution modal is temperature dependent. It is almost mono-modal distribution (uniform distribution) in compacts sintered at 1200 °C (Fig. 16b) and 1300 °C (Fig. 16d), whereas the bi-modal and multi-modal pore size distributions were obtained in those sintered at 1250 °C (Fig. 16c) and 1000 °C (Fig. 16a), respectively. It should be mentioned that even though the modal of pore size distribution is the same (homogeneous) for samples sintered at 1200 and 1300 °C, they may behave differently. In fact, the large interval of pore size distribution (0.1–10 μm) in samples sintered at 1200 °C is shifted towards a narrow interval of pore size distribution (8–50 μm). On the basis of the above results, it can be said that the increase in sintering temperature encourages the coalescence of pores, which in turn, leads to a larger average pore size (Table 2).

These kinds of pore size distribution curves do not tell us more information about both cumulative porous volume (%) and average pore size (μm). Consequently, curves of cumulative porous volume (%) versus pore diameter were re-plotted in Figs. 17–20, using four different processing routes.

It should be mentioned that the average pore size is directly given by mercury intrusion porosimetry. Moreover, these values are in good agreement with those determined also from

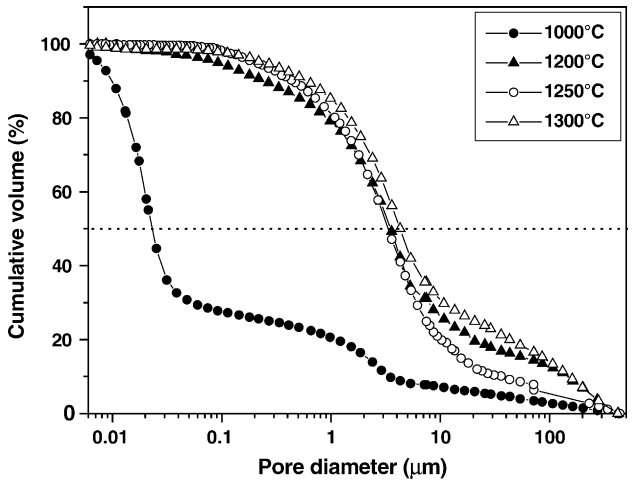

Fig. 17. Cumulative porous volume (%) as a function of pore size for kaolin samples, sintered at different temperatures for 1 h, using process 1.

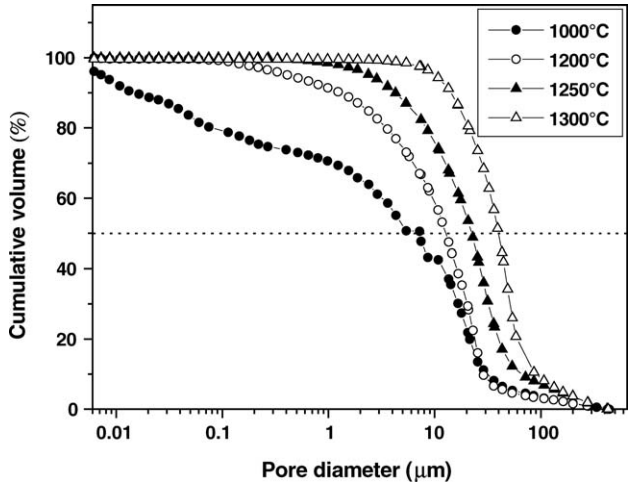

Fig. 18. Cumulative porous volume (%) as a function of pore size for kaolin + 15 wt% doloma samples, sintered at different temperatures for 1 h, using process 2.

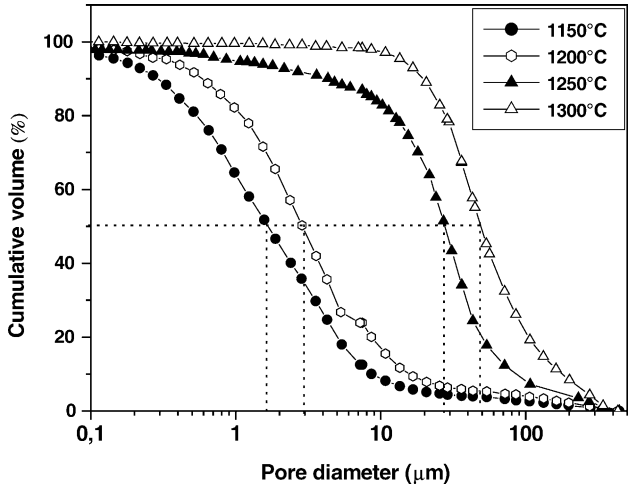

Fig. 19. Cumulative porous volume (%) as a function of pore size for kaolin + 15 wt% doloma samples, sintered at different temperatures for 1 h, using process 3.

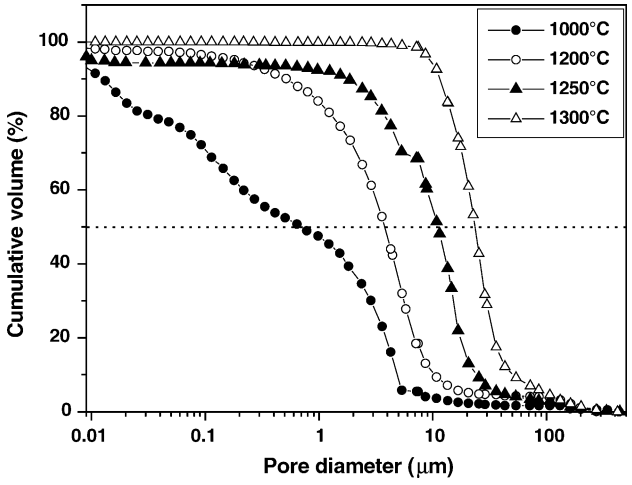

Fig. 20. Cumulative porous volume (%) as a function of pore size for kaolin + 15 wt% doloma samples, sintered at different temperatures for 1 h, using process 4.

the pore size corresponding to 50% of cumulative volume (Figs. 17–20).

These figures show mainly that the average pore size is shifted towards higher values when sintering temperature is increased. For example, the average pore size values in samples sintered at 1150, 1200, 1250 and 1300 °C, using process 3 were 2, 3, 27 and 50 μm, respectively. These values correspond to a cumulative porous volume = 50% (in Fig. 19). Furthermore, these curves may inform us about the percentage (%) of any pore size interval, at a given sintering temperature and processing route. In some applications this information is required.

All in all, it can be said that each processing route has its advantages and potential uses.

3.4. Tensile strength

A typical curve of the tensile strength of samples, prepared according to process 4 (Fig. 3) as a function of sintering temperature is shown in Fig. 21. This figure shows that there are three different stages (domains). Following an initial rapid increase in tensile strength, a state of constant tensile strength is reached for samples sintered at temperatures ranged between 1200 and 1250 °C. Afterwards, the tensile strength decreased sharply for samples sintered at 1300 °C.

A careful examination of the figures, concerning pores characterization, shows that the tensile strength may be controlled by many factors. Consequently, a general correlation seems to exist between densification, microstructural changes (average pore size, pore distribution and total porosity) and tensile strength in sintered compacts as follows:

1– Densification and grain size are the dominant factors controlling strength, since most of the total pores were intergranular, e.g., the substantial increase in strengths of samples corresponded to a parallel increase in density which means a decrease in porosity ratio (stage 1).

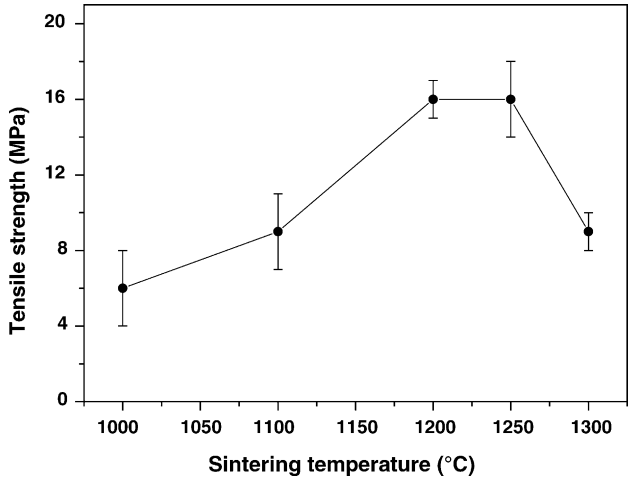

Fig. 21. Tensile strength as a function of sintering temperature for kaolin + 15 wt% doloma compacts, using process 4.

2– Consistently, the relatively higher constant strengths (stage 2) were occasioned by high relative densities and pore size factors. This means that densification enhances tensile strength whereas pores coalescence acts oppositely on it.
3– Pore size and distribution influenced by sintering temperature is a factor controlling strength. A good example is shown in Figs. 16d and 20 for compacts sintered at 1300 °C for 60 min. Therefore, pores coalescence becomes a predominant factor in this stage (stage 3).

4. Conclusions

The attractiveness in the present work is the development of membrane supports manufactured from native kaolin and doloma (obtained from dolomite) mixtures, available in our country. This kind of supports presents features of porosity (porous volume and average pore size) more important than those elaborated from kaolin as a raw material. They can be used as supports of membranes of microfiltration and ultrafiltration. Moreover, these supports are characterised by a reduced manufacture cost since the used raw materials are very abundant (in Algeria) and their mechanical properties seem to be acceptable. The manufactured membrane supports are mainly constituted of mullite, cordierite and anorthite phases. The presence of these phases may also extend further their use, even under severe atmosphere conditions. Finally, it has been found that the pore structures (modal distributions of pore size, total porosity and average pore size) may be controlled by the sintering temperature, additions and processing routes. For examples, a uniform pore size distribution within a total porosity ratio of 43% and 28 μm as an average pore size, were obtained, for samples prepared according to process 3 and sintered at 1250 °C for 1 h. However, a relatively higher porosity ratio (51%) was reached when process 2 was applied, under the same sintering conditions.

References

1. Lee, S. H., Chung, K. C., Shin, M. C., Dong, J. I., Lee, H. S. and Auh, K. H., Preparation of ceramic membrane and application to the cross flow microfiltration of soluble waste oil. *Mater. Lett.*, 2002, **52**, 266–271.
2. Gaucher, C., Jaouen, P., Comiti, J. and Legentilhomme, P., Determination of cake thickness and porosity during cross-flow ultrafiltration on a plane ceramic membrane surface using an electrochemical method. *J. Membr. Sci.*, 2002, **210**, 245–258.
3. Gestel, T. V., Vandecasteele, C., Buekenhoudt, A., Dotremont, C., Luyten, J., Leysen, R. *et al.*, Alumina and titania multilayer membranes for nanofiltration: preparation, characterization and chemical stability. *J. Membr. Sci.*, 2002, **207**, 73–89.
4. Lenza, R. F. S. and Vasconcelos, W. L., Synthesis and properties of microporous sol–gel silica membranes. *J. Non-Cryst. Solids.*, 2000, **273**, 164–169.
5. Romanos, G. E., Steriotis, Th., A., Kikkinides, E. S., Kanellopoulos, N. K., Kasseelouri, V. *et al.*, Innovative methods for preparation and testing of Al_2O_3 supported silicalite-l membranes. *J. Eur. Ceram. Soc.*, 2001, **21**, 119–126.
6. Zhong, S. H., Li, C. F. and Xiao, X. F., Preparation and characterization of polyimide–silica hybrid membranes on kieselguhr–mullite supports. *J. Membr. Sci.*, 2002, **199**, 53–58.
7. Saffaj, N., Younssi, S. A., Albizane, A., Messouadi, A., Bouhria, M., Persin, M. *et al.*, Preparation and characterization of ultrafiltration membranes for toxic removal from wastewater. *Desalination*, 2004, **168**, 259–263.
8. Mohammadi, T. and Pak, A., Effect of calcination temperature of kaolin as a support for zeolite membranes. *Sep. Purif. Technol.*, 2003, **30**, 241–249.
9. Rakib, S., Sghiar, M., Rafik, M., Cot, D., Larbot, A. and Cot, L., Elaboration et caractérisation d'une céramique macroporeuse à base d'arène granitique. *Ann. Chim. Sci. Mat.*, 2000, **25**, 567–576.
10. Elmoudden, N., Elghazouali, A., Rakib, S., Sghyar, M., Rafiq, M., Larbot, A. *et al.*, Nouveaux supports membranaires à base de chamotte d'argile. *Ann. Chim. Sci. Mat.*, 2001, **26**(2), 5–11.
11. Harabi, A., Mecif, A., Achour, A. and Barama, S. E., Effect of chemical composition on sintering and mechanical properties of local kaolin. In *Ninth CIMTEC Proceedings, Ceramics: Getting into the 2000's, part B*, ed. P. Vincenzini, 1999, pp. 871–878.
12. Harabi, A., and, S. and Achour, A., A process for sintering of MgO and CaO based ceramics. *J. Mater. Sci. Lett.*, 1999, **18**, 955–957.
13. Harabi, A., *Studies of an alumina-chromia system containing mullite*. PhD thesis, Manchester Materials Science Centre, UMIST, Manchester, UK, 1990.